ELSEVIER

European Polymer Journal 38 (2002) 25–31

EUROPEAN POLYMER JOURNAL

www.elsevier.com/locate/europolj

Geometrical stability and energy storage of some conducting large aromatic sulfonate-doped polyaniline

Seddique M. Ahmed *, Saleh A. Ahmed

Department of Chemistry, Faculty of Science, Assiut University, 71516 Assiut, Egypt

Received 4 April 2001; received in revised form 22 June 2001; accepted 26 June 2001

Abstract

Incorporation of large aromatic sulfonate (AS) into polyaniline emeraldine base form (PANI-EB) was investigated. Geometrical stability of AS-doped polyaniline was confirmed by molecular modeling calculations. The energy storage (ES) ($W\,h\,kg^{-1}$) of these polymers depends on the size of the AS and the functional group in the dopant. Cyclic voltammetric measurements showed that the electroactivity of the AS-doped PANI, due to the oxidation/reduction of the first redox only of the salt/base PANI. A good linearity between the cathodic peak height (I_{pc1}) and the square root of the scan rate ($\sqrt{v}$) more than 0.95 over the range 5–100 $mV\,s^{-1}$ indicate the electron transfer is diffusion controlled.

Keywords: Molecular modeling calculations; Geometrical stability; Aromatic sulfonates; Polyaniline; Doping level; Energy storage

1. Introduction

Theoretical predictions for various neutral and charged forms of polyaniline were studied [1]. The MNDO semiempirical calculations [2] for polyaniline as base polymer is an insulator with a large bandgap. Oxidation of this material produces radical cations on the chains. This oxidation has also been described as two electron process for yielding dications (or bi-polarons) on the chain with the following structure:

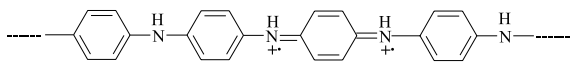

This doubly charged defect with its quinoid linkage is analogous to the dication or bi-polaron species identified spectroscopically in several aromatic containing polymer systems [3,4].

In this study, molecular modeling calculations showed that the geometrical configuration of (PANI-EB) doped with large aromatic sulfonate (AS) is highly stable.

Polymers with π-conjugated bonds show uncommon properties like low energy electronic transition, low ionization potential, and high electronic affinity. These properties mean the polymer can be easily oxidized and reduced. To compensate the charge in the polymer matrix, there is incorporation or explusion of ionic species (dopants) whose chemistry can affect the redox process and modify the physicochemical properties of the polymers, like its conductivity. Among conducting polymers, PANI has been studied due to its potential applications, such as optoelectronic chemical sensors, corrosion inhibitor, rechargeable lithium batteries, etc. [5–13]. The main problem related to lithium battery is the majority participation of anions in the charge compensation properties [14]. This produces a diminution of less than 30 $W\,h\,kg^{-1}$ for the PANI-Li system [15]. This is related to different types of configuration for batteries using conducting polymers as a cathode. An increase in the energy density can be expected if the polymer uses cations

* Corresponding author.

E-mail addresses: sm_ahmed@yahoo.com (S.M. Ahmed), saleh_63@hotmail.com (S.A. Ahmed).

0014-3057/01/$ - see front matter
PII: S0014-3057(01)00179-3

rather than anions for charge compensation process [16, 17].

The currently used cathodes are metallic oxides such as Mn_2O_4 or V_6O_{13} with Li^+ intercalated into the van der Waals gaps [14]. Cathode based on conducting polymers usually show poor capacities so that the available power from their electrochemical systems is insufficient for practical applications. Higher current capability requires faster redox switching, which in PANI is often associated with the transport of both anion and cation inside the polymer matrix [15]. Great reversibility of the redox system can thus be expected if the ionic conductivity of PANI is enhanced without sacrificing its electronic properties.

Recently, we have reported that the electrical properties and conductivity of some PANI derivatives and polypyrrole colloids (base form) were enhanced after doping [19–21]. In this work, conducting polyaniline without external acid doping was made by incorporating large AS. In addition, geometrical stability of AS-doped PANI was confirmed by molecular modeling calculations. Energy storage (ES) ($W\,h\,kg^{-1}$) of AS-doped PANI was determined coulometrically in aqueous medium containing 10% dimethylsulfoxide (DMSO), pH = 2.13, adjusted by $HClO_4$, 100 mM benzenesulfonate (BS). All researches before this work, used PANI as a film or as a colloidal particles using stabilizer [17, 21–28].

2. Experimental

Aniline and DMSO were used as purchased from Merck (reagent grade). All ASs were added as sodium salt (Aldrich, reagent grade). All other chemicals and reagents were used as received. Bidistilled water was used throughout.

Emeraldine base form of (PANI-EB) was synthesized by the use of chemical oxidation method of Cao and coworkers [29]. The colloidal particles of *m*-nitrobenzene sulfonate (*m*-NBS)-doped PANI were also synthesized by the chemical oxidation of aniline in the presence of a steric stabilizer (polyvinyl alcohol, PVA) [30]. FT-IR Spectroscopic measurements in KBr pellets were carried out using a Shimadzu (Type 470) spectrometer.

Molecular modeling calculations (MM+) was carried out using Hyper Chem program Version 5 (Polak-Ribiere PM5). Thermogravimetric/mass analysis were performed with a Jeol MS-TG/DTA (Model 220) under He atmosphere. A given amount of *m*-NBS-doped PANI was placed in a sample holder, and the temperature was changed from 40°C to 610°C at the programmed heating rate of 5°C/min. Elemental analysis for C, H, N were carried out by using Elementer analysensysteme (GmbH, Donaustr-7, D-63452) Hanau, Germany.

All the electrochemical measurements were referred to an Ag|AgCl|saturated KCl||electrode, and planar glassy carbon electrodes (Tokai grade GC-30, 3 mm in diameter) were used in cyclic voltammetric experiments. A sheet of NISSINBO AC-140 glassy carbon (2.9 cm^2), which was a gift from Nihon Postal Franker Co., was used as a working electrode for coulometric experiments. Voltammetric measurements were carried out at ambient temperatures (25 ± 1°C) with a data acquisition system constructed in our laboratory. Electrolysis efficiency more than 98% was obtained with this electrode for reduction of 4 mM $[Fe(CN)_6]^{3-}$ at 0.5 $ml\,min^{-1}$. The experimental procedures have reported in detail [21,30].

3. Results and discussion

3.1. Molecular modeling calculations of AS-doped PANI

Molecular modeling calculations (MM+) showed a geometrical energy of PANI (EB) dimer of 1.41 $kcal\,mol^{-1}$ and gradiant 0.0762. This means the geometrical configuration of this dimer is highly stable (Fig. 1a). We also found that AS-doped with PANI (Table 1) was highly stable with energy between 46.63–101.53 $kcal\,mol^{-1}$ (Fig. 1b). MM+ calculations indicated that the lowest energy structures of AS-doped PANI had a doping level of 50%. There were other possible configurations but they were less stable. The torsion angle (dihydral angle) between the planes of adjacent rings of PANI is difficult to calculate because, at the MNDO level of approximation, there is not much energy associated with the torsion. Both PANI(EB) dimer form (DPANI-EB) and $PANI^{++}$ $2H/2AS^-$ optimize with PM5 to 90° torsion angles and a C–N–C bond angle of 127°. DPANI-EB optimizes to a torsion angle of 70°; however, this value is quite sensitive to the details of how the molecular topology and symmetry are specified to the MM+ program. This is due to the softness of the force constant associated with the torsional motion of the adjacent rings; the different between a 90° twist and a 30° twist is only about 3 $kcal\,mol^{-3}$. The MM+ calculations for AS-doped PANI are summarized in Table 1. From the energy data listed in Table 1 it is clear that the geometrical stability of the optimum configuration structures of the dopants or composites (PANI/AS) are highly dependent on the both position and size of the substituents in the dopant according to the following scheme:

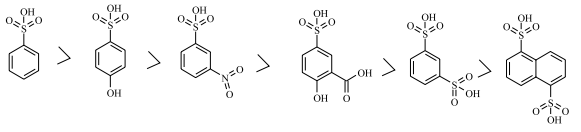

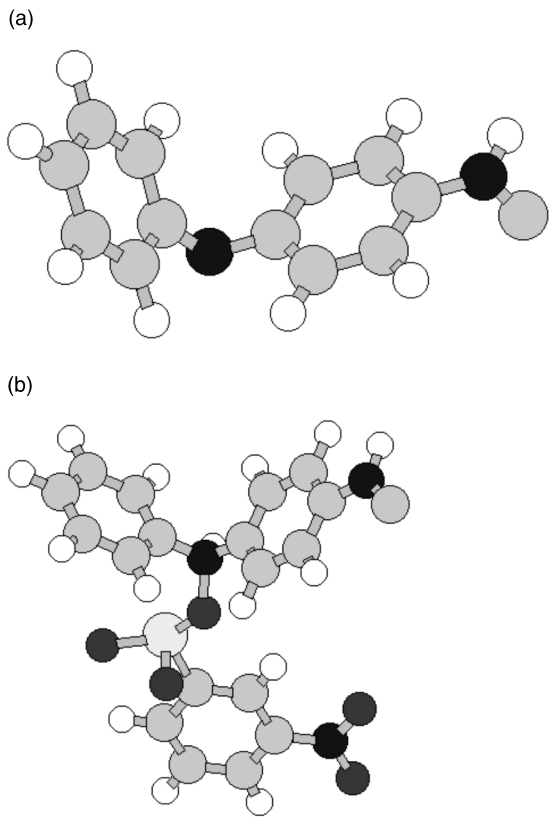

Fig. 1. (a) Molecular modeling optimization of the dimer form of PANI(EB) and (b) Molecular modeling optimization of the dimer form of PANI (*m*-NBS).

Table 1
Geometrical energy and gradient of the optimum configuration structures of the dopants and AS-doped PANI

No.	Composite (PANI/AS)	Energy (kcal mol^{-1})	Gradient
1	PANI(EB-dimmer) (ANI)	1.41 (2.14)	0.0762 (0.0988)
2	PANI/BS (BS)	46.64 (6.85)	0.0953 (0.0963)
3	PANI/*p*-OH–BS (*p*-OH–BS)	47.39 (6.96)	0.0869 (0.0889)
4	PANI/*m*-NBS (*m*-NBS)	50.38 (9.54)	0.0934 (0.0871)
5	PANI/5-SSA (5-SSA)	51.38 (15.16)	0.0846 (0.0939)
6	PANI/*m*-BDS (*m*-BDS)	88.75 (16.45)	0.0965 (0.0747)
7	PANI/1,5-NDS (1,5-NDS)	101.54 (17.73)	0.0900 (0.0938)

ANI, aniline; PANI, polyaniline as a dimmer form; *p*-OH–BS, *p*-hydroxy benzene sulfonate; 1,5-NDS, 1,5-naphthalene disulfonate; *m*-NBS, *m*-nitrobenzene sulfonate; *m*-BDS, *m*-benzene disulfonate; PVA, polyvinyl alcohol; 5-SSA, 5-sulfosalyclic acid; BS, benzene sulfonate.

3.2. Characterization of m-nitrobenzene sulfonate-doped PANI

FT-IR spectra of *m*-NBS and *m*-NBS-doped PANI give clear evidence for the protonation of (PANI-EB). In these spectra the peaks appearing at ~1610 and 1533 cm^{-1} as doublets are due to the asymmetric stretching vibration of the –NO_2 group [31], whereas the peaks at 910 and 880 cm^{-1} are due to the C–N stretching of the aromatic nitro compound [18]. The bands at 1220 and 1190 cm^{-1} are due to SO_3^- groups [32].

The FT-IR spectrum of *m*-NBS-doped PANI exhibits some interesting features in comparison that of (PANI-EB) and *m*-NBS. The peaks at ~1600 and 1500 cm^{-1} are ascribed to quinoid and benzenoid rings of PANI-EB respectively [30]. The wave numbers are shifted to 1565 and 1485 cm^{-1}, respectively, for *m*-NBS-doped PANI. Such red shifts indicate the delocalization of quinoid and benzenoid structures to the semiquinoid form (polaron) in the polymer chain, confirming the protonation of the emeraldine base [30]. The ratio of benzenoid to quinoid form was lower for *m*-NBS-doped PANI than for PANI-EB, revealing again the semiquinoid form. In fact, the intensity of the quinoid form should be larger than that of the benzenoid form in the case of *m*-NBS-doped PANI, since the peak at ~1565 cm^{-1} should be piled up with that of –NO_2 group appearing at ~1610 cm^{-1}. The peak at 1045 cm^{-1} is attributed to the symmetric and antisymmetric stretching modes of SO_3^- group [32].

The thermal behavior of *m*-NBS-doped PANI is depicted along with the DTG curves in Fig. 2. The DTG curve clearly indicates a three-step decomposition process. The initial weight loss (1.18%) is attributed to the desorption of superficial water molecules associated with the doped PANI. The mass spectra presented in Fig. 3(t_1) reveal an intense fragment of the water molecule at m/z, 18. The *m*-NBS-doped PANI then remains stable until ~144°C. The second step, extending up to ~260°C with the weight loss of 18.89% (Fig. 3(t_2)), indicates the loss of sulfinyl (SO^+, m/z, 48), sulfonyl SO_2^+, m/z, 64). The appearance of a fragment of m/z, 18, arises from the strongly bound water molecules associated with the dopant. The fragments at m/z, 78, and m/z, 93, are due to C_6H_6 and $C_6H_5NH_2$, and suggest that polymer chain degradation occurs. At higher temperature (Fig. 3(t_3)) the fragments are probably from the decomposition of the polymer backbone and the dopant. PANI is thermally unstable above ~144°C. Evidently, thermal processing is not profitable but solution electrochemistry is promising.

Elemental analysis of *m*-NBS-doped PANI also indicated the inclusion of *m*-NBS in the polymer chain (% found: C: 55.10; H: 3.90; N: 11.08; S: 8.13 and O: 21.06). Consequently, we can safely conclude from the results of MM+ calculations, FT-IR, TG/mass and elemental

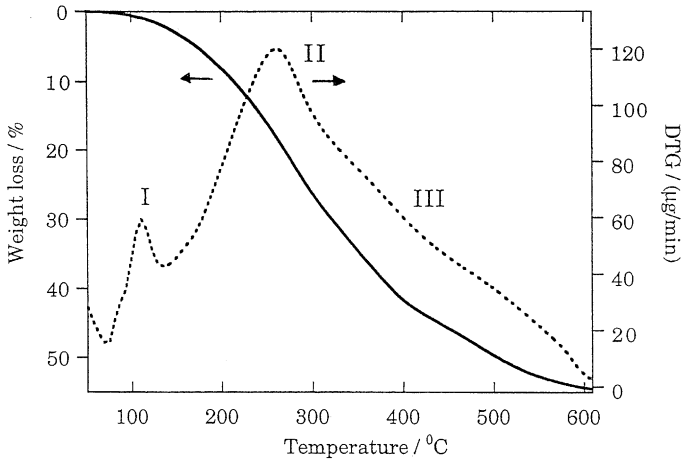

Fig. 2. Thermal pattern of *m*-NBS-doped PANI. Heating scan rate 5°C/min.

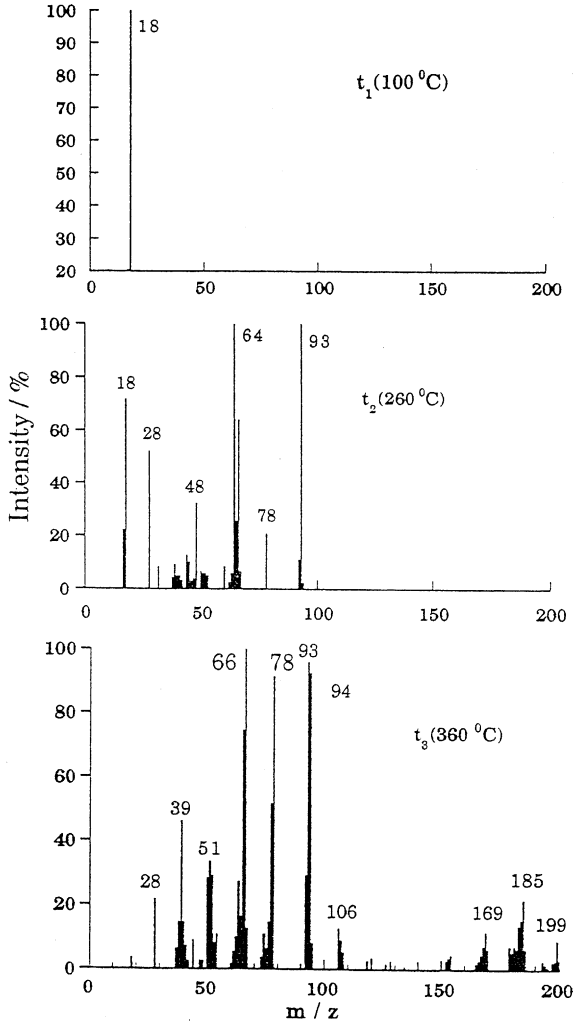

Fig. 3. Mass spectra of *m*-NBS-doped PANI taken at different temperatures.

analysis that the PANI was doped with *m*-NBS with doping level 50% as shown in Fig. 1b.

3.3. Electroactivity of PANI enhanced after doping by AS

The electroactivity of benzenesulfonic acid-doped PANI has been investigated by Nagaoka et al. [33]. They showed that the first and second redox of BS-doped PANI is very small compared with the present study. The electroactivity of (*p*-OH–BS)-doped PANI is due to the first redox as shown in Fig. 4a. This means that the electron transfer of *p*-OH–BS-doped PANI might be fast. The reason might be due to the hydroxyl group enhancing the release of protons from the SO_3H groups. A good linearity between the reduction peak height ($r > 0.95$) of the first redox (Fig. 4b) of *p*-OH–BS-doped PANI and the square root of scan rate ($\sqrt{v}$) in the range (5–100 $mV\,s^{-1}$) suggested that the dissolved AS-doped PANI composite did not adsorb on the electrode surface.

3.4. Energy storage of some conducting AS-doped PANI

The electroactivity of conducting polymers is very important for many possible applications such as ES [34], antistatic coatings [17] etc. The theoretical capacity ($W\,h\,kg^{-1}$) of the energy can be calculated if the weight (W or $Mwt\,kg^{-1}$) of the electroactive species is known [35].

$$Q = mF(W/Mwt) \tag{1}$$

$$Q = \frac{n(As)(W\,kg^{-1}/Mwt)}{3600} = A\,h\,kg^{-1} \tag{2}$$

If the applied voltage (V) during charge (oxidation) or discharge (reduction) are known, the ES will be.

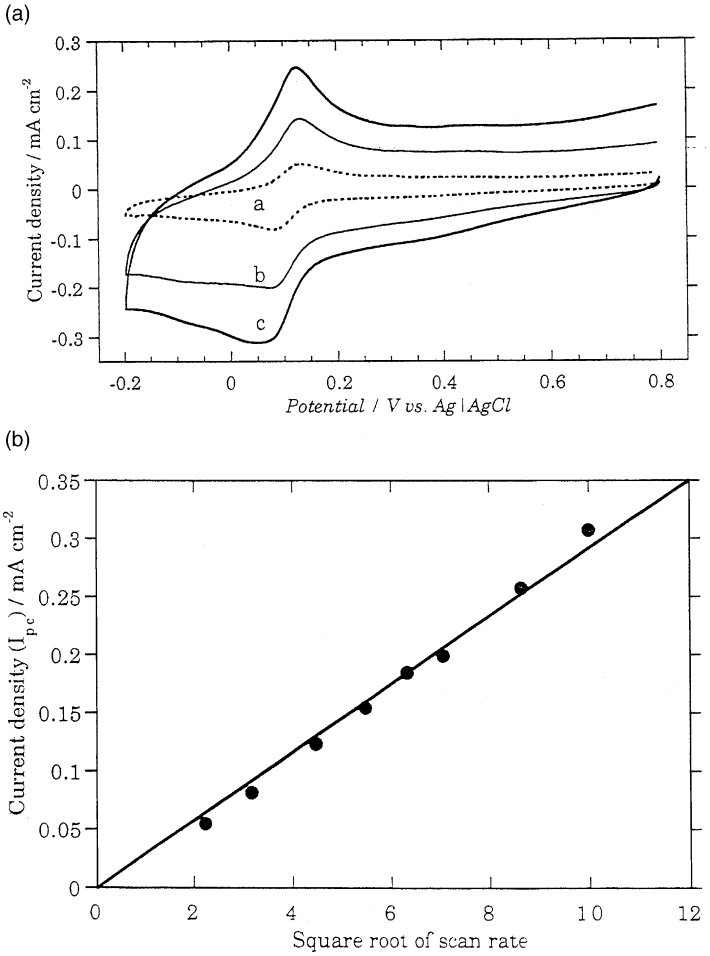

Fig. 4. (a) Cyclic voltammograms of 200 mg l^{-1} of *p*-OH–BS-doped PANI base electrolyte (BE): 100 mM benzenesulfonate (BS), pH 2.13 ($HClO_4$), in aqueous medium containing 10% DMSO. Scan rates a, b and c are 10, 50 and 100 mV s^{-1}; (b) Cathodic peak height (I_{pc1}) vs. square root ($\sqrt{v}$) of (a).

$$ES = Q(\mathrm{A\,h\,kg^{-1}})|V| = \mathrm{W\,h\,kg^{-1}} \quad (3)$$

where: Q, is a charge; n, number of electrons; F, Faraday constant.

The ES of AS-doped PANI also could be calculated experimentally using the following equations [33]:

$$Q = \int_{t=0}^{t=\infty} I\,\mathrm{d}t \quad (4)$$

$$ES = Q(\mathrm{A\,h\,kg^{-1}})|V| = \mathrm{W\,h\,kg^{-1}} \quad (5)$$

Fig. 5 shows that the reduced *p*-OH–BS-doped PANI has the ability to store about 27.67 W h kg^{-1} in a condensed lightweight form. Table 2 shows the ES of some conducting AS-doped PANI samples. From this Table, the highest energy is associated with *p*-OH–BS-doped PANI. The reason is not yet clear but perhaps the –OH (electron donating group) is responsible for the increasing release of protons from the sulfonic acid groups and is thus responsible for higher than mineral acids [36,37]. The ES in *m*-BDS-doped PANI is about four times higher than in colloidal particles of *m*-BDS-doped PANI (PVA). The reason might be that polymeric stabilizers in the first layer of the colloids act as insulators towards electron transfer [38,39].

4. Conclusions

Molecular modeling calculations indicate that the geometrical configuration of AS-doped polyaniline is highly stable with a doping level of 50%. The electroactivity of PANI is enhanced by doping with AS derivatives. The energy consumed during electrolysis of these doped polymers depends on the size and the substituted groups.

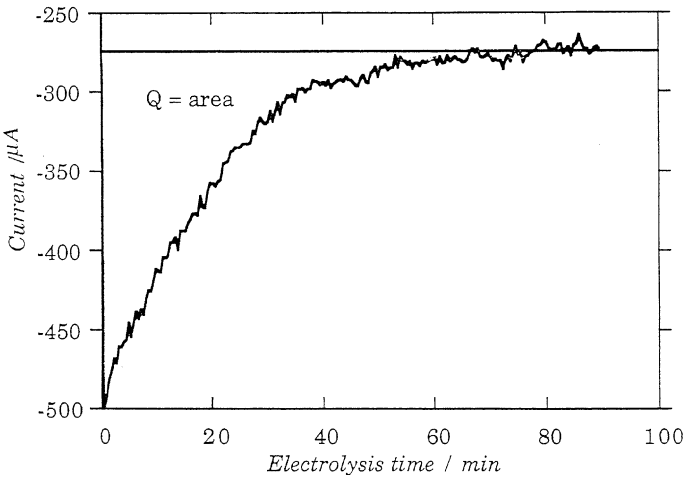

Fig. 5. Electrolysis of 100 mg l^{-1} of *p*-OH–BS-doped PANI at +0.4 V vs. Ag|AgCl electrode. BE: 100 mM BS, pH 2.13 ($HClO_4$) in aqueous medium containing 10% DMSO.

Table 2
Values of the ES of some conducting large AS doped PANI samples

Composite PANI/AS	ES (W h kg^{-1}) Theoretical	ES (W h kg^{-1}) Observed	% of ES (Observed/ theoretical)
PANI/*p*-OH–BS	120.81	27.67	22.91
PANI/1,5-NDS	94.68	13.62	14.39
PANI/*m*-NBS	111.68	11.04	9.89
PANI/*m*-BDS	102.36	9.12	8.91
PANI(PVA)/*m*-BDS	97.25	2.56	2.63
PANI/5-SSA	107.49	6.90	6.42
PANI/BS	165.59	1.19	0.72
Lead-acid battery [30]	161.00	~30.00	18.63

Acknowledgements

We are grateful to the faculty members of the chemistry department, Assiut University for their encouragement.

References

[1] Chance RR, Bouudreaux DS, Wolf JF, Shacklette IW, Silbey B, Themans B, Andre JM, Bredas JL. Synth Met 1986;15:105.
[2] MacDiarmid AG, Chiang JC, Halpern M, Huang WS, Mu SL, Somasiri NLD, Wu W, Yaniger SI. Mol Cryst Liq Cryst 1985;121:137.
[3] Dewar MJS, Thiel W. J Am Chem Soc 1977;99:4899.
[4] Dewar MJS, Thiel W. J Am Chem Soc 1977;99:4907.
[5] Scrosati B. In: Scrosati B, editor. Application of electroactive polymers. New York: Chapman and Hall; 1993.
[6] Inzelt G. Electroanalysis 1995;7:895.
[7] Genies EM, Hany P, Santier Ch. J Appl Electrochem 1988;18:751.
[8] Kitani A, Yano J, Sasaki K. J Electroanal Chem 1986;209:277.
[9] Dhawan SK, Trivedi DC. Polym Int 1991;25:55.
[10] Bartlett PN, Patricia BMA, Sim KLC. Sens Acutuators 1989;19:125.
[11] Sathiyanarayanan S, Dhawan SK, Trivedi DC, Balakrishnan K. Corros Sci 1992;33:1831.
[12] Inzelt G. In: Bard AJ, editor. Electroanalytical chemistry, vol. 18. New York: Marcel Dekker; 1996. p. 89.
[13] Kameko M, Woehrle D. Advances in polymer science. Berlin: Springer; 1988. p. 141.
[14] Desilvestro J, Scherfele W, Haas O. J Electrochem Soc 1992;139:2727.
[15] Barbero C, Miras MC, Schnyder B, Haas O, Kotz R. J Mater Chem 1994;4:1775.
[16] Barbero C, Miras MC, Kotz R, Haas O. Synth Met 1993;55–57:1539.
[17] Varela H, Torresi RM. J Electrochem Soc 2000;147(2):665.
[18] Bruce PG, editor. Solid state electrochemistry. Cambridge, UK: Cambridge University Press; 1995.
[19] Ahmed SM, Patil RC, Nakayama M, Ogura K. Synth Met 2000;114:156.
[20] Patil RC, Ahmed SM, Shiigi H, Nakayama M, Ogura K. J Polym Sci: Part A: Polym Chem 1999;37:4596.
[21] Nagaoka T, Ahmed SM, Ogura K. J Electrochem Soc 1999;146(9):3378.
[22] Bjarklund RB, Liedberg B. J Chem Soc, Chem Commun 1986:1239.

[23] Armes SP, Aldissi M, Agnew SF, Gottes S. Langmuir 1990;6:1745.
[24] Cawdery N, Obey TM, Vincent B. J Chem Soc, Chem Commun 1988:1189.
[25] Digar ML, Bhattafcharyya SN, Mandal BM. J Chem Soc, Chem Commun 1992:18.
[26] Aldissi M. Adv Mater 1993:5:60.
[27] Stejskal J, Kratochvil P. Langmuir 1996;12:3389.
[28] Stejskal J, Kratochvil P. Polym Int 1993;32:401.
[29] Cao Y, Smith P, Heeger AJ. Synth Met 1989;32:263.
[30] Aldissi M. Adv Mater 1993;5:60.
[31] Harada I, Furukawa Y, Ueda F. Synth Met 1989;E-303:29.
[32] Bellamy LJ. In the infrared spectra of complex molecules. London: Chapman and Hall; 1975. p. 75, 131, 408.
[33] Nagaoka T, Nakao H, Suyama T, Ogura K. Anal Chem 1997;69:1030.
[34] Olcani A, Abe M, Ezo M, Doi T, Miyata, Miyak A. Synth Met 1993;3696:57.
[35] Hibbert DB. Introduction to electrochemistry. University of New South Wales, Australia, 1993. p. 298.
[36] Wang ZH, Ray A, MacDiarmid AG, Epstein AJ. Phys Rev B 1991;43(5):4373.
[37] Wang YZ, Joo J, Hus CH, Epstein AJ. Synth Met 1995;69:267.
[38] Chen Z, Okimoto A, Nagaoka T. Anal Chem 1999;71:1834.
[39] Luk SY, Lineton W, Keane M, Dearmitt C, Armes SP. J Chem Soc, Faraday Trans 1995;91:905.